

# Velocity Control Mechanism of the Under-actuated Hammering Robot for Gravity Compensation

Yusuke Takahashi<sup>a</sup>, Satoru Nakamura<sup>a</sup>, Yasuichi Ogawa<sup>b</sup> and Tomoya Satoh<sup>b</sup>

<sup>a</sup>Tokyu Construction Co.,Ltd.

<sup>b</sup>Ogawayuki Co.,Ltd.

E-mail: takahashi.yuusuke@tokyu-cnst.co.jp

## Abstract -

According to rapid deterioration of many domestic tunnels and bridges, engineers that manage them are insufficient. For this reason, it is desired to develop an automatic hammering robot that can inspect them quickly and accurately. If hammering sounds of this robot are similar to those of engineers, we can do it by using experience for a long period. Therefore, we developed an under-actuated hammering robot that can simulate hammering sounds by engineers. However this robot have a problem that it cannot generate same sounds because of the effect of gravity. To this problem, we combined a swing slider crank mechanism, and controlled velocity of the hammer according to gravity. In this paper, we described the under-actuated hammering robot that combined a swing slider crank mechanism and its model. After that, we clarified a velocity control mechanism for gravity compensation. Finally, we showed the result of hammering tests using this robot and verified usefulness of this mechanism.

## Keywords -

Concrete inspection; Hammering robot; Under-actuated; Gravity compensation

## 1 Introduction

Many domestic tunnels and bridges that was built at a period of rapid economic growth in Japan have deteriorated over time. In Japan, there were 100 thousand road tunnels at the time of March 2013. In particular, 20% of these tunnels have passed over 50 years and it is estimated that it will be 50% in 20 years[1]. Moreover, it was enforced new road laws in July 1, 2014 that obliged to do a close up visual inspection and a hammering to the concrete delamination every 5 years, and we are demanding these inspection more accurately. On the other hand, engineers that manage them are insufficient. For this reason, it is desired to develop innovative inspection techniques such as robots and to implement them on site.

Systems that find out concrete cracks using a digital camera or others are actually implemented on site[2]. Furthermore, there are delamination detection systems for concrete, for example, a system using an infrared camera is considered. However, this system has a problem that accuracy of detection varies as the environmental condition. As the delamination detection technique, hammering test method is widely been accepted. We can find out a delamination inside the concrete by hammering the concrete

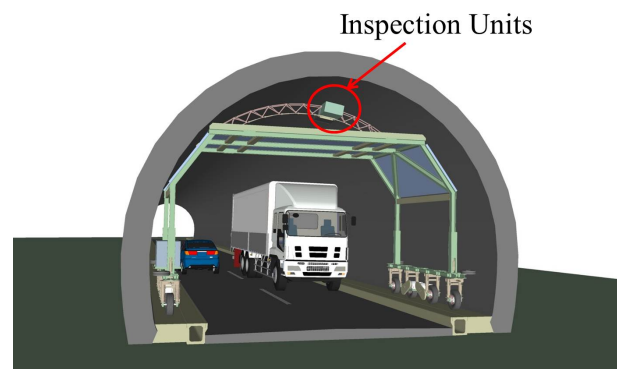


Figure 1. Image of the Tunnel Inspection System

surface[3]. For example, referring to “douro tonnel teiki tenken youryou” (that is a Japanese road tunnel inspection guideline) which was enforced by a ministry of Japan, a sound concrete sounds like a high note and a delaminated concrete sounds like a low note. If the hammering robot sounds like human, engineers can inspect those in accordance with the guideline.

In this research, we aim to develop robots which can sound like human, and we developed an under-actuated hammering robot with a hammer swing mechanism (hereinafter, this is called “Under-actuated system”) that behaves similar to that of an engineers arm[4]. We aim to inspect tunnel automatically by using vehicles such as Figure 1 equipped this robot. However, this system allows the hammer to rotate freely, so there is a possibility that the robot cannot sound as the same sound. Therefore, we controlled velocity of the hammer by a swing slider-crank mechanism (“Slider-crank system”).

In this paper, we first described the under-actuated hammering robot that combined a slider-crank system and its model. After that, we clarified a velocity control mechanism for gravity compensation. Finally, we showed the result of hammering tests using this robot and verified usefulness of this mechanism.

## 2 Underactuated Hammering Robot

An important point to imitate the robot’s hammering sound to engineer’s one is not to press the hammer against

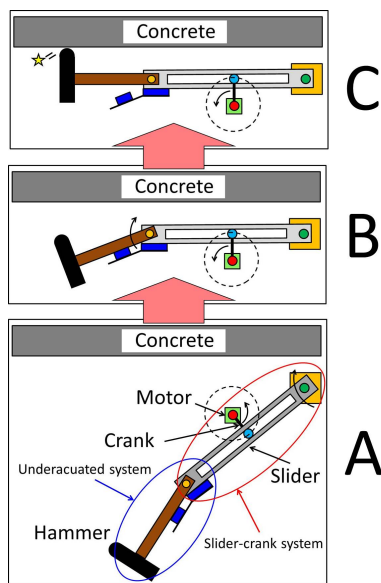


Figure 2. Behavior of the underactuated hammering robot

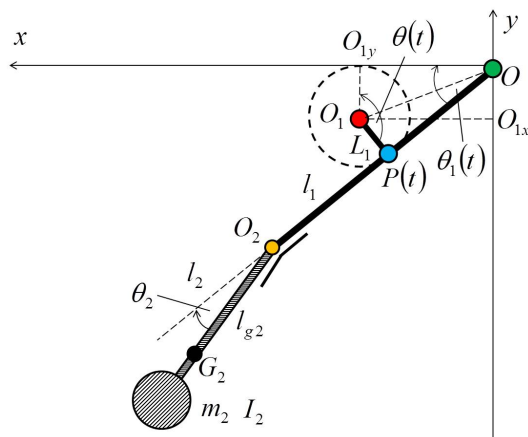


Figure 3. Model of the underactuated hammering robot



Figure 4. The underactuated hammering robot

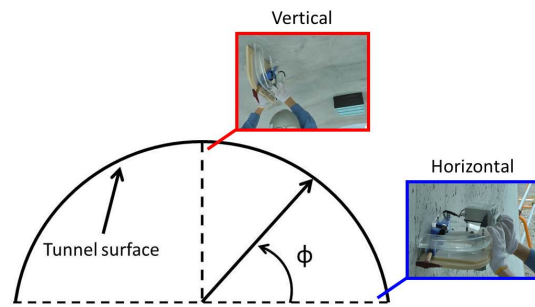


Figure 5. Definition of  $\phi$

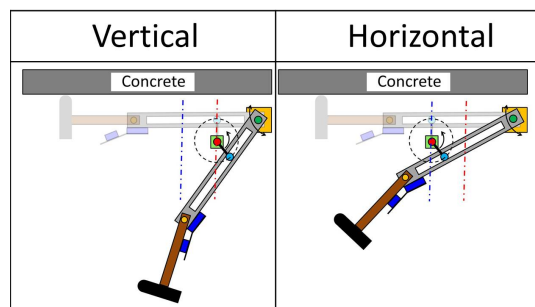


Figure 6. Method of gravity compensation

the concrete surface[5]. The reason is that it does not suppress the vibration of concrete and not occur a double hammering. Furthermore, in this research, we hypothesize that it is also important point to reproduce the behavior of a engineers arm, especially snap wrist. As a hammering robot of satisfying these points, we invented a mechanism that combined a under-actuated system with a slider-crank system. Image of this robot's behavior is shown in Figure 2, and it's model of the mechanism is shown in Figure 3. If the motor at  $O_1$  rotates at  $N$  [rpm], a crank( $O_1P$ ,  $L_1$  [m]) rotates at  $O_1$ , and a slider( $OO_2$ ,  $l_1$  [m]) swing around  $O$ . This showed A and B in Figure 2. There is a hammer( $L_2$  [m],  $m_2$  [kg],  $I_2$ [g·mm<sup>2</sup>]) at  $O_2$ , and it limits counterclockwise rotation by the stopper. After that, if a slider decelerates as showed C, this hammer accelerates and hammering at  $x$ -axis. This behavior is similar to snap wrist when engineers are hammering, and we think that it is effective for detecting a delamination inside the concrete. Because this hammer leaves concrete by elasticity, it does not suppress the vibration of concrete and not occur a double hammering. We developed a robot based on these method and showed it in Figure 4, it's specification showed Table 1.

### 3 Velocity Control Mechanism

As this under-actuated system has a characteristic that hammer rotates freely, kinetic energy becomes decrease by the effect of gravity. It means that hammering sounds become small. To be similar to engineers sounds, it should

maintain kinetic energy a constant and gets same sounds. Therefore, we invented a velocity control mechanism that controls position  $O_1$  according to gravity.

In this section, we described advantages and behavior of this mechanisms. After that, we showed a dynamical model of this robot and verified numerically.

### 3.1 Axis Position Control Method

As a method to maintain kinetic energy of the hammer a constant, it is easiest to control velocity of the hammer according to gravity. For example, if defining the hammering direction  $\phi$ [deg] (as showed in Figure 5),  $N$ [rpm] increases according to  $\phi$ [deg] and kinetic energy increases. However, this method has disadvantage because it means that inspection speed slows down in the horizontal direction. Moreover, there is a possibility that engineers cannot detect correctly because if  $N$ [rpm] changes and hammering pitch changes. From these problem, we invented a velocity control mechanism that controls motor position  $O_{1y}$ [mm] according to  $\phi$ [deg]. This mechanism showed in Figure 6. For example, if  $O_{1y}$ [mm] decreases (or  $O_1$  approaches  $O$ ), swing angle of slider increases and velocity of a hammer also increases. Therefore, it can be made constant of kinetic energy of the hammer by controls velocity of a hammer as described. This mechanism has another advantage that hammering pitch is constant and inspection speed does not slow down because it is not necessary to change  $N$ [rpm].

### 3.2 Control Theory

To control velocity of a hammer according to  $\phi$ [deg], we aimed to get relation between  $\phi$ [deg] and  $O_{1y}$ [mm] from a dynamical model of the robot. In Figure 3,  $\theta(t)$ [deg] is the right-handed system, and  $\theta_1(t)$ [deg],  $\theta_2(t)$ [deg] is a left-handed system. Equation of motion of hammer can be written as

$$A(t)\ddot{\theta}_1(t) + B\ddot{\theta}_2(t) + H(t) + G(t) = 0 \quad (1)$$

where,

$L_1, O_{1x}$	10 [mm]	$l_1$	90 [mm]
$l_2$	120 [mm]	$m_2$	133.8 [g]
$I_2$	$131.6 \times 10^3$ [g·mm <sup>2</sup> ]	$\theta_2$	20 [deg]
$N$	180[rpm]		

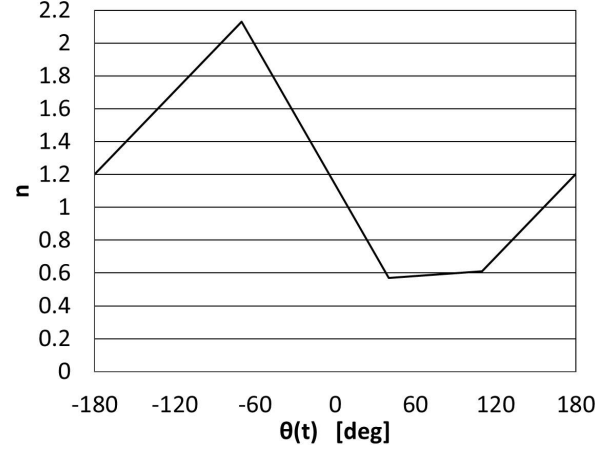


Figure 7. Gear ratio of the motor

$$\begin{aligned} A(t) &= m_2 l_{g2}^2 + I_2 + m_2 l_1 l_{g2} \cos \theta_2(t) \\ B &= m_2 l_{g2}^2 + I_2 \\ H(t) &= m_2 l_1 l_{g2} \dot{\theta}_2(t)^2 \sin \theta_2(t) \\ G(t) &= m_2 (g \cos \phi) l_{g2} \cos (\theta_1(t) + \theta_2(t)) \end{aligned} \quad (2)$$

To get sufficient velocity for hammer when hammering, this robot has special gears which reduction ratio is  $n$  as shown in Figure 7. When  $\theta_1(t)$ [deg] is written by

$$\theta(t) = \int \frac{2\pi n}{60} N dt \quad (3)$$

The relationship between  $\theta_1(t)$ [deg] and  $\theta(t)$ [deg] is obtained geometrically

$$\begin{aligned} \theta_1(t) &= -\angle O_{1y} O O_1 + \angle O_1 O P \\ &= -\tan^{-1} \left( \frac{L_1}{O_{1y}} \right) + \sin^{-1} \left( \frac{L_1}{P(t)} \sin \theta(t) \right) \end{aligned} \quad (4)$$

where

$$P(t) = \sqrt{L_1^2 + L_2^2 - 2L_1 L_2 \cos \theta(t)} \quad (5)$$

$$L_2 = \overline{O O_1} = \sqrt{O_{1x}^2 + O_{1y}^2} \quad (6)$$

From Equation (3) and (5), we let  $\theta_1(t)$ [deg] be an input. Therefore, we transform  $\theta_1(t)$ [deg] as an input and  $\theta_2(t)$ [deg] as an output,

$$\ddot{\theta}_2(t) = -\frac{1}{B} (A(t)\ddot{\theta}_1(t) + H(t) + G(t)) \quad (7)$$

To analyze the motion of hammer, we should solve Equation (7) for  $\theta_2(t)$ [deg]. However, it is difficult to

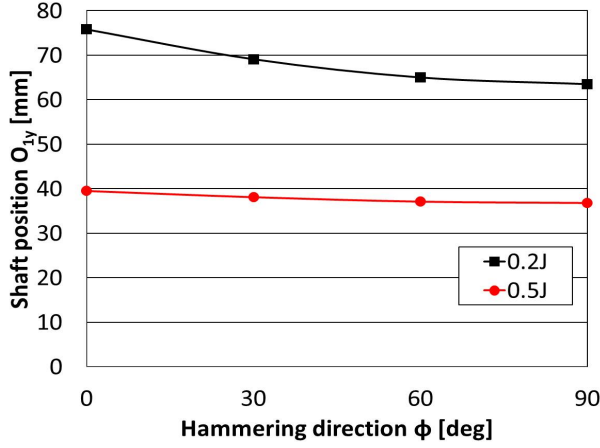


Figure 8. Hammering direction vs Shaft position

get analytical solution because this equation is non-linear. Therefore, we analyze it numerically by the Euler method. The pitch width is

$$\Delta t = t_{n+1} - t_n \quad (8)$$

and we can get numerical solution as follows

$$\dot{\theta}_2(t_{n+1}) = \dot{\theta}_2(t_n) + \ddot{\theta}_2(t_n)(t_{n+1} - t_n) \quad (9)$$

$$\theta_2(t_{n+1}) = \theta_2(t_n) + \dot{\theta}_2(t_n)(t_{n+1} - t_n) \quad (10)$$

when initial conditions are

$$\dot{\theta}_2(t_0) = \dot{\theta}_2(0) = 0 \quad (11)$$

$$\theta_2(t_0) = \theta_2(0) = 0 \quad (12)$$

kinetic energy of the hammer  $E$ [J] is written by

$$E = \frac{1}{2}m_2l_1^2\dot{\theta}_2^2 + m_2l_1l_{g2}\dot{\theta}_1(\dot{\theta}_1 + \dot{\theta}_2)\cos\theta_2 + \frac{1}{2}(m_2l_{g2}^2 + I_2)(\dot{\theta}_1 + \dot{\theta}_2)^2 \quad (13)$$

Actually, considering the machine loss  $L_1 = 0.2$ [%],

$$E_1 = (100 - L_1) \times 0.01 \times E \quad (14)$$

For example, in Table 1, relationship between  $\phi$ [deg] and  $O_{1y}$ [mm] to maintain energy of 0.2[J] or 0.5[J] is shown as in Figure 8.

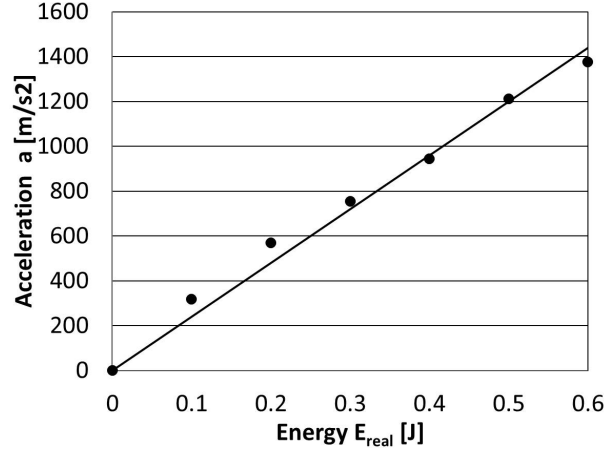


Figure 9. Energy of the steel ball vs Acceleration of the wood



Figure 10. measuring device

## 4 Hammering Experiment

In this section, we showed the result of hammering tests using this robot and verified usefulness of this theory. We first described how to estimate kinetic energy of the hammer. After that, we described about experimental procedure. Finally, we compare the results obtained from the experiment with the theory.

### 4.1 Estimation Method of Physical Energy

Vibration is generated when collides one with another. Therefore, we expected that kinetic energy correlates with vibration acceleration. From this expectation, we experimented that a steel ball with a weight of 94.9[g] dropped freely from various heights and collided with a stationary wood, and plotted relationship between kinetic energy of a steel ball and vibration acceleration of a wood. To detect acceleration, we used the piezoelectric acceleration pickup (PV-95, Rion Co.,Ltd.) and observed by FFT analyzer. The experiment was repeated 5 times and the ball dropped to the same point. The experimental result is shown in Figure 9. From Figure 9, plots are found to be almost linear. Linear approximate equation obtained by least-square method is as follows

$$E_{real} \approx \frac{1}{2397}a \quad (15)$$

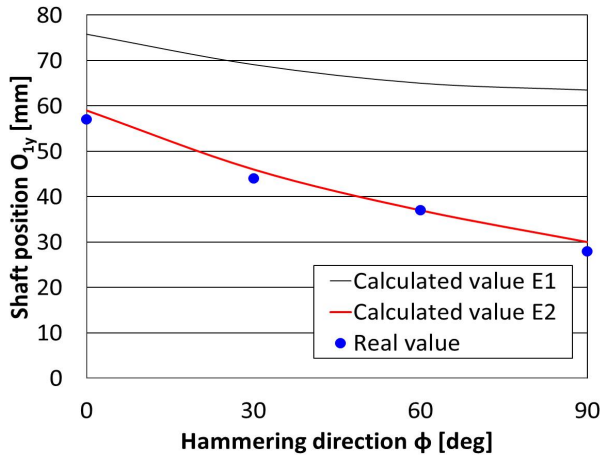


Figure 11. Hammering direction vs Shaft position at 0.2[J]

Therefore, we can estimate kinetic energy of the hammer by Equation (15).

#### 4.2 Experimental Procedure

We developed a rotating device as shown in Figure 10 and attached a hammering robot, and estimated kinetic energy of the hammer by Equation (15). We experimented at 0[deg], 30[deg], 60[deg], 90[deg] and the axial position was adjusted to keep kinetic energy of the hammer. Considering that we aim to develop robots which can sound like human in this research, hammering energy should be the same as engineers. Therefore, we measured hammering energy of them, sound area is 0.5[J] and delamination area is 0.2[J]. However, we cannot obtain the repetition at 0.5[J] because the plastic deformation occurred in a part of the wood. This problem can be resolved by using stainless, but the acceleration is too high and we cannot observe it by device we possess. Therefore, in this research, we experimented at 0.2[J] which assumed delamination area. This experiment was repeated 5 times.

#### 4.3 Experimental Results and Consideration

Relationship between theoretical energy E1 and experimental energy shown as Figure 11. As shown in Figure 11, theoretical energy and experimental energy are not corresponded. Comparing theoretical energy between experimental energy, for example,  $O_{1y}$  is 17[mm] at 0[deg], and 33[mm] at 90[deg]. For this reason, it is expected energy loss by a collision between hammer and stopper. In Figure 2-C, hammer which rebounded from concrete collides a stopper in Figure 2-A. Hammer can get reaction force and accelerate if it is on stopper in Figure 2-B. However, if it cannot get sufficient reaction force by this collision, actual kinetic energy of a hammer is more poor.

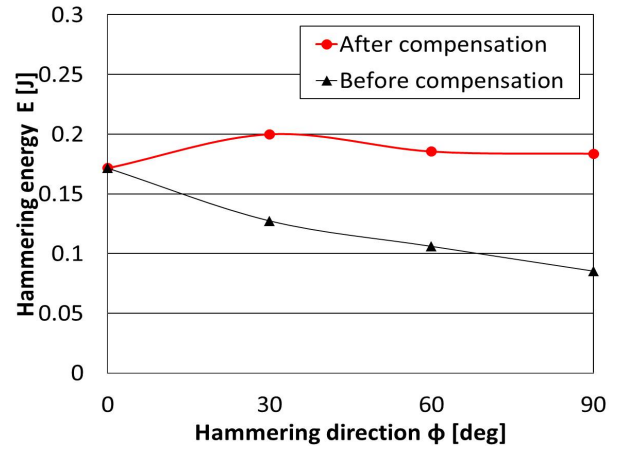


Figure 12. Hammering direction vs Hammering energy

It is expected that the more influence of the weight of a hammer (that is hammering direction) greater, the more energy decreases. Therefore, defining loss  $L_2$  [%] with  $\phi$  [deg] as a variable,

$$L_2 = 15 \sin \phi \quad (16)$$

In this experiment, we found out phenomenon that the more  $O_1$  approaches  $O$ , the more load of the motor increase. Therefore, defining loss  $L_3$  [%] with  $O_{1y}$  [mm] as a variable,

$$L_3 = \frac{1300}{O_{1y}} \quad (17)$$

We incorporate Equation (16) and (17) into (14) and correct it shown as

$$E_2 = (100 - (L_1 + L_2 + L_3)) \times 0.01 \times E \quad (18)$$

Figure 11 shows theoretical energy E2 by Equation (18). As shown in Figure 11, theoretical energy and experimental energy are almost match.

To verify usefulness of technique that we invented, we compared the case of changing  $O_{1y}$  [mm] according to E2 (that say after compensation) and the case of not changing it (that say before compensation). Result of this is shown in Figure 12. As shown in Figure 12, it can maintain 0.2[J] in the case of after compensation. On the other hand, in the case of before compensation, the more  $\phi$  [deg] increases, the more energy decreases, especially 0.09[J] at 90[deg].

## 5 Conclusion

In this research, we aim to develop robots can sound like human hammering, and we developed an under-actuated hammering robot that combined an under-actuated system which behaves similar to that of engineers arm and

slider-crank system. In this paper, we described this robot and its model. After that, we clarified a velocity control mechanism for gravity compensation. Finally, we showed the result of hammering test using this robot and verified usefulness of this mechanism. As a result of the test, theoretical energy and experimental energy are almost corresponded by considering energy loss that occur by collision of hammer and stopper and changing the motor position. Furthermore, the robot which applied this method and mechanism can hammering with constant kinetic energy. For future work, we will develop moving devices which is equipped with hammering robots and aim for practical use for hammering test in tunnels and bridges.

## 6 Acknowledgements

This work was in part supported by Council for Science, Technology and Innovation, “Cross-ministerial Strategic Innovation Promotion Program (SIP), Infrastructure Maintenance, Renovation, and Management” (funding agency: NEDO).

## References

- [1] Ministry of Land, Infrastructure and Transport in Japan. “Present state of road structure for aging countermeasure of road (tunnel)”. [http://www.mlit.go.jp/road/sisaku/yobohozen/yobo1\\_1.pdf](http://www.mlit.go.jp/road/sisaku/yobohozen/yobo1_1.pdf)
- [2] Masato Ukai and Kazuya Shimoda. “Tunnel Delineation Inspection System Using Line Sensor Camera”. <http://jcma.hetempl.jp/bunken-search/wp-content/uploads/2011/11/035.pdf>
- [3] Manabu Takeishi and Kazuhiro Koizumi. “Automatic Hammering Survey System IDATEN”. <http://jcma.hetempl.jp/bunken-search/wp-content/uploads/ronbun/2004/043.pdf>
- [4] Yusuke Takahashi and Satoru Nakamura. “Control Method of the Underactuated Hammering System considering Concrete Sound”. ROBOMECH2016, 2A2-09a6, 2016.
- [5] Yasuo Mori, Takayuki Iwai. “Development of Tunnel Lining Hammering Sound Diagnostic System”. <http://jcma.hetempl.jp/bunken-search/wp-content/uploads/ronbun/2004/042.pdf>
- [6] Yusuke Takahashi and Satoru Nakamura. “Development of the Hammering System with Underactuated Mechanism for Tunnel Inspection and Evaluation of Performance”. Construction Robot Symposium, 2015.